Journal of Mining Science, Vol. 45, No. 5, 2009

MODELING THE ELASTIC WAVE PROPAGATION IN A BLOCK MEDIUM UNDER THE IMPULSE LOADING

N. I. Aleksandrova, M. V. Ayzenberg-Stepanenko*, and E. N. Sher UDC 622.7 + 622

The wave propagation analysis revealed that the low-frequency pendulum wave propagating in a 2D block medium with periodic structure due to the action of local impulse has a two-wave structure. The shape of such wave depends on its propagation direction. Modeling the blast-induced seismic wave propagation in a two-layer block rock mass with the weak upper layer and stiff lower layer showed that the far distant point from the wave excitation source is first reached by the small amplitude pendulum wave running in the stiffer lower layer and then by the delayed maximum-amplitude wave propagating in the upper layer.

Elastic wave, block rock mass, impulse loading, pendulum wave, two-layer medium

Down to recent times, the rock mechanics and geophysics have extensively been using a theory that a rock mass deforms as a uniform medium dynamics of which is described by the linear theory of elastic wave propagation. The latter theory grounded methodological outlines for stress calculation in rocks with excavations, as well as for seismic data processing and interpretation in geoexploration and mining.

The recent investigations motivate the reconsideration of the prevailing opinions by pointing at the block structure of rock masses to be taken into account in mathematical models of geomechanical and seismic events. These studies have highly been inspired by Sadovsky's fundamental concept on block hierarchy structure of geomedium objects [1]. By this concept, a rock mass is a system of different scale nested rock blocks bonded via bands of weaker jointy rocks. Both in statics and dynamics, a block rock mass generally deforms due to the deformation of these pliable bands.

The structural inhomogeneity causes different dynamic events absent in a uniform medium, for instance, pendulum-type elastic wave propagation in periodic-structured rock masses [2].

According to the theoretical and experimental research of wave propagation in the one-dimensional block medium models [3 – 9], by representing blocks as massive nondeformable bodies, it is possible to separate out a part of an elastic block medium, which is governed by deformation of inter-block bands. The impact load generates a strain wave that contains low-frequency pendulum-type waves characterized by (a) relatively long duration the impulse excitation being short, (b) substantially lower velocity than the velocity of elastic waves in a medium made of material of blocks and (c) weak attenuation.

The measurements of seismic waves generated by blasting at open pits show that, as a rule, the travel time of a signal grows as the signal propagates and the share of the low frequency oscillations enlarges.

As an illustration of the aforesaid, Fig. 1 shows seismic oscillation velocities in soil, in orthogonally related directions (*XYZ*), obtained during a blast at Iskitimizvest JSC Open Pit, 1850 m away of the blasted rock block site.

Institute of Mining, Siberian Branch, Russian Academy of Sciences, Novosibirsk, Russia. *Ben-Gurion University, Beer-Sheva, Israel. Translated from Fiziko-Tekhnicheskie Problemy Razrabotki Poleznykh Iskopaemykh, No. 5, pp. 21-32, September-October, 2009. Original article submitted August 10, 2009.

1062-7391/09/4505-0427 ©2009 Springer Science + Business Media, Inc.

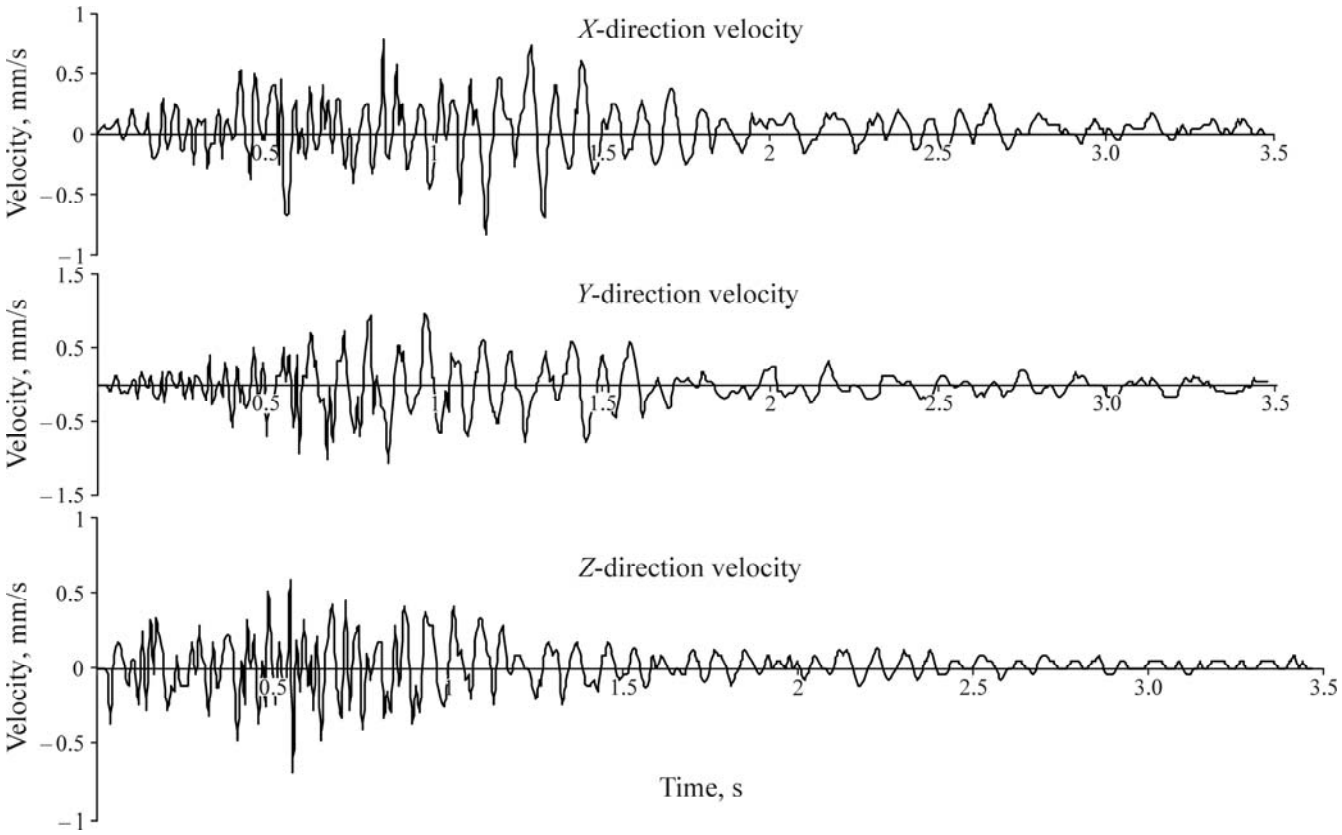

Fig. 1. Seismic oscillations under blasting at Iskitimizvest JSC Open Pit on Sep 25, 2006, distant by 1850 m from the blast site

A rock block was shot with a 1-s short-delay single blast. Oscillations in soil continued over 1 s, with a lower frequency than under the blast (Fig. 1). This suggests the wave dispersion in the block medium and emergence of the low-frequency pendulum-type waves with lower velocities than those of P-waves. In this connection, it is important to analyze the wave propagation in a spatial block medium model under the impact loading.

This paper describes the two-dimensional modeling of seismic wave propagation under explosion in a uniform or layered block medium. Similarly to the works [10, 11], the block medium dynamics is considered in a pendulum approximation when the blocks are assumed incompressible and the displacements are due to the compression of bands. The simplest calculation model in this case is a regular lattice of masses connected by elastic springs. The same study in the one-dimensional case showed that the "mass-and-spring chain" model sufficiently describes the low-frequency wave propagation in a one-dimensional block medium composed of elastic rods and separation layers, in a definite range of stiffness.

Wave Propagation in 2D Infinite Lattice. The theory of waves in periodic structures ensued from Rayleigh's classical study [12] relies on the thorough research [13 – 16] and is continuously developing. The theory has found application in the mechanics of composite structures and composite materials [17 – 20], is of use in designing different filters — structures endowed with band spectrum: zones of transmission and blockage of elastic, acoustic and electromagnetic waves [21]. It is challenging to apply the theory to describing the seismic response of a block medium to the impulse excitation.

The 2D anti-plain strain study involves a square lattice of point masses M connected by springs of length L, the springs possess equal stiffness k in either direction (Fig. 2).

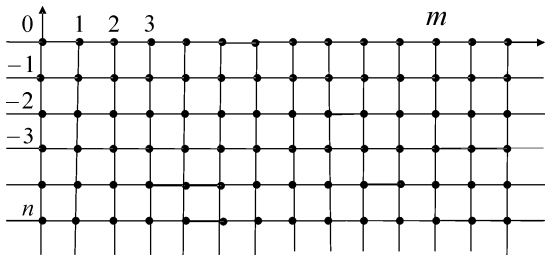

Fig. 2. The model of a square lattice of masses and springs

The motion equations for this system have the form:

$$M\ddot{u}_{m,n} = k(u_{m+1,n} + u_{m-1,n} - 4u_{m,n} + u_{m,n+1} + u_{m,n-1}) + Q(m,n,t), \quad (n \le 0, \ m \ge 0). \tag{1}$$

Here, $u_{m,n}$ is the displacement of the masses in orthogonal direction relative to the plane of the lattice; m and n are the number of the masses in x- and y-directions, respectively; $Q(m,n,t)$ is the effective load at point (m, n).

The mass (0, 0) at the initial moment experiences the half-sine load:

$$Q(0,0,t) = Q_0 \sin(\omega_* t) H \ (\pi - \omega_* t), \tag{2}$$

where H is the Heaviside step function; ω_* is the disturbing frequency.

Initial conditions are zero. Boundary conditions correspond to the process symmetry relative to axes x and y:

$$u_{-1,n} = u_{1,n} \quad (n \le 0), \quad u_{m,1} = u_{m,-1} \quad (m \ge 0). \tag{3}$$

The system of Eqs. (1)–(3) is solved by the finite difference method. For the second time derivate, the central difference second-order accuracy approximation is used. Then the homogenous difference system of equations to conform to the initial system (1) acquires the form:

$$M(u_{m,n}^{s+1} - 2u_{m,n}^{s} + u_{m,n}^{s-1}) = \tau^2 k(u_{m+1,n}^{s} + u_{m-1,n}^{s} - 4u_{m,n}^{s} + u_{m,n+1}^{s} + u_{m,n-1}^{s}). \tag{4}$$

Here, $u_{m,n}^{s}$ is $u_{m,n}(t)$ in the time layer s ($t = s\tau$, τ is the time step, $s = 0, 1, 2, \ldots$). The zero initial conditions are approximated by the central differences: $u_{m,n}^{-1} = u_{m,n}^{1}$. The stability condition for the resultant finite difference relations is $\tau\sqrt{2k/M} \le 1$.

Consider dispersion features of the homogenous system (1). The harmonic wave propagation in this system is governed by the relation:

$$\omega = \omega_0 \sqrt{4 - 2\cos k_x - 2\cos k_y}, \quad \omega_0 = \sqrt{k/M}, \tag{5}$$

where k_x and k_y are the x-component and y-component of the wavevector $\boldsymbol{k}$. As shown in [22], there are two resonant frequencies in the system under analysis: $\omega_1 = 2\omega_0$ ($k_y = \pm\pi \pm k_x$ and $k_y = k_x = \pm\pi$). The frequency ω_2 corresponds to the edge of the transmission band ($\omega < \omega_2$) and the blockage band ($\omega > \omega_2$), and has an analog in the one-dimensional case, while ω_1 is in the transmission band and has no analog in the one-dimensional case. Under the action of a local monochromatic disturbance with frequency ω_1, the pronounced spatial directedness features the resonant wave propagation: the large part of energy concentrates along diagonals and has the group velocity $c_1 = L\sqrt{k/2M}$ [22, 23]. The resonant process at ω_2 has no pronounced directedness. As in the homogenous medium, the low-frequency wave propagates every way with the same velocity (phase and group), $c = L\sqrt{k/M}$.

The impulse excitation complicates the spatial wave pattern. Based on the analysis of the calculations of (1) – (3), correlate propagations of the disturbances generated by the monochromatic and impulse sources.

Figures 3 and 4 exemplify the estimated relationships between mass velocities, time and spectral densities $G(\omega) = \left| \int_0^T \dot{u}_{m,n} e^{-i\omega t} dt \right|$ at different spatial points, under the impulse excitation. The problem parameters: $M = 1, L = 1, k = 1, \omega_* = 10, T = 150, \tau = 0.07$. In Fig. 3 — $m = 20$, $n = 0$; in Fig. 4 — $m = 20$, $n = -20$.

Figure 3*a*: the first vertical dashed line in the velocity oscillogram corresponds to the arrival time $t_1 = m/c$ of the horizontal pendulum-type wave propagating with the low velocity $c = L\sqrt{k/M} = 1$ from the disturbance source to the point (*m*, 0). It is followed up by the slower velocity, modulated packet of oscillations, and the mean amplitude of the first modulation is twice as large the first modulation in the pendulum wave. The high-frequency packet amplitude gets smaller in time but still is comparable with the pendulum wave amplitude for a sufficient time interval. The numerical experiments showed that the second packet velocity is associated with the diagonal propagation of the wave group with the resonant frequency ω_1. The second vertical dashed line in Fig. 3*a* denotes the second wave packet arrival time t_2, diagonally propagating with the velocity $c_1 = c/\sqrt{2}$ ($t_2 = \sqrt{2}m/c_1 = 2m/c$). Likewise, the two-wave pattern exists in the diagonal direction (Fig. 4*a*). Though in this case, the pendulum wave is recorded at the very beginning of the oscillations (the first vertical dashed line in Fig. 4*a*, for $t_1 = m\sqrt{2}/c$). Comparatively shortly (the second dashed line, $t_2 = 2m/c$), the larger amplitude high-frequency packet arrives, the frequency being close in value to $\omega = 2$.

The described pattern correlates with the oscillation spectra (Figs. 3*b* and 4*b*): in the relatively low frequency interval ($\omega \le 1.5$), the spectra in the two cases analyzed differ slightly, and the pendulum wave share is basically the same. The difference grows with the higher frequency: there is a pronounced peak in the second case at the resonant frequency $\omega_1 = 2$, which explains the large share of oscillations with this frequency. The value $\omega = 2\sqrt{2}$ is the upper edge of the frequency transmission band. At this edge, the spectrum densities reach their maxima in the horizontal and vertical directions from the excitation point (Fig. 3*b*) at the high-frequency impulse $\omega_* = 10$.

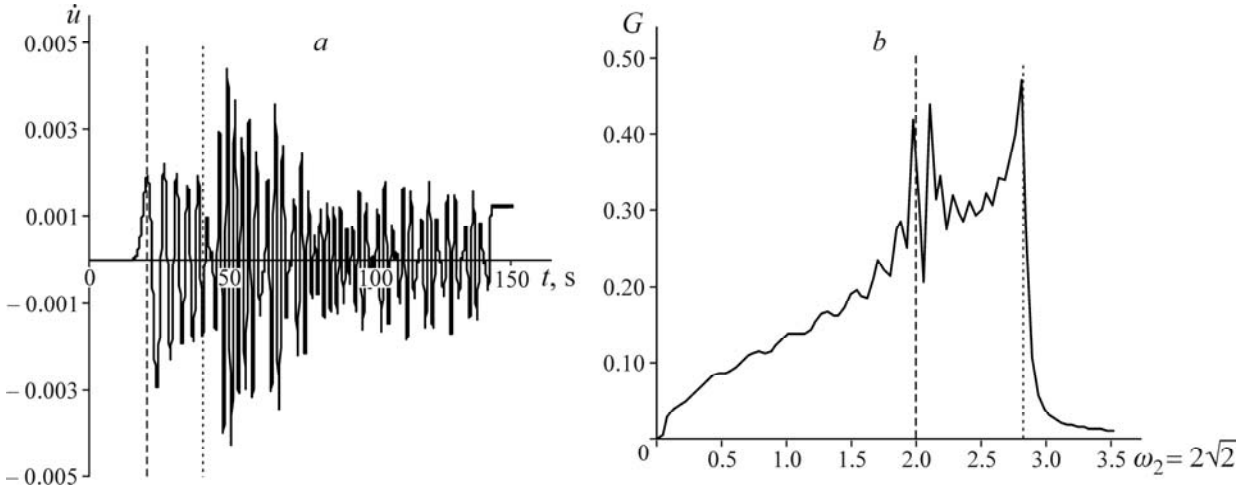

Fig. 3. (*a*) Velocity of point mass (20, 0) versus time; (*b*) point mass (20, 0) spectral density versus frequency of impact loading applied to point mass (0, 0)

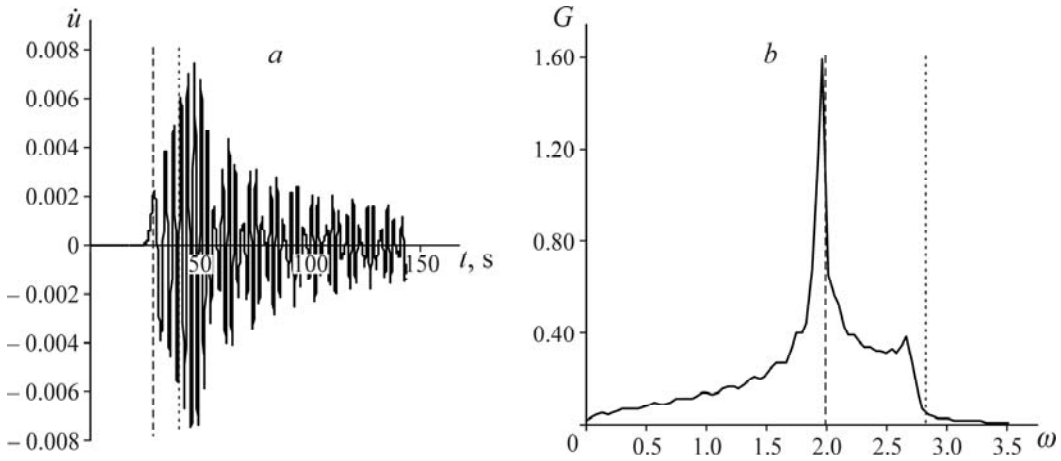

Fig. 4. (*a*) Velocity of point mass (20, – 20) versus time; (*b*) point mass (20, – 20) spectral density versus frequency of impact loading applied to point mass (0, 0)

Wave Propagation in a Layered Block Medium. Blasting at open pits originates a layered block medium. Upper parts of a treated horizon are destructed by previous blasts; these horizons are modeled by a lattice with lower value stiffness than for the bottom parts. Consider the wave propagation in a two-layer block mass on a stiff base; the block mass stiffness is the same in both directions and differs in the layers (Fig. 5).

The mass motion equations have the form:

$$M\ddot{u}_{m,n} = k_1(u_{m+1,n} - 2u_{m,n} + u_{m-1,n}) + k_1(u_{m,n+1} - 2u_{m,n} + u_{m,n-1}) + Q(m,n,t),\ (m \geq 0,\ 0 \geq n \geq n_1 + 1),$$

$$M\ddot{u}_{m,n} = k_2(u_{m+1,n} - 2u_{m,n} + u_{m-1,n}) + k_2(u_{m,n+1} - 2u_{m,n} + u_{m,n-1}) + Q(m,n,t),\ (m \geq 0,\ n_1 - 1 \geq n \geq n_2 + 1), \quad (6)$$

$$M\ddot{u}_{m,n_1} = \frac{k_1 + k_2}{2}(u_{m+1,n_1} - 2u_{m,n_1} + u_{m-1,n_1}) + k_1(u_{m,n_1+1} - u_{m,n_1}) + k_2(u_{m,n_1-1} - u_{m,n_1}) + Q(m,n_1,t).$$

In layer $0 \geq n \geq n_1$ spring stiffness in both directions is k_1 and in layer $n_1 \geq n \geq n_2$ is k_2.

The boundary conditions agree with the symmetry relative to axis *y*:

$$u_{-1,n} = u_{1,n} \quad (n = 0, ..., n_2) \tag{7}$$

and with the bind when $n = n_2$:

$$u_{m,n_2+1} = 0 \quad (m = 0, ..., \infty). \tag{8}$$

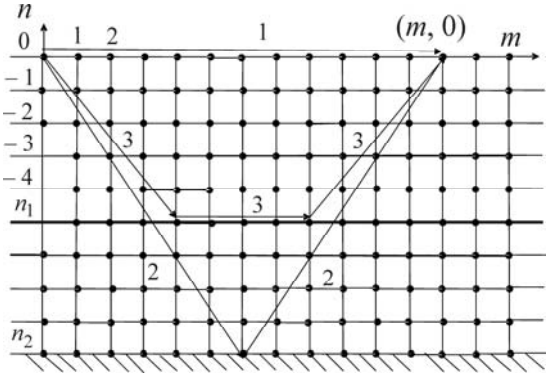

Fig. 5. Layered block medium lattice and passages of seismic wave fronts. The load application is at point mass (0, 0), recording is at point mass (*m*, 0)

For $n = 0$ it is assigned that y-directed stresses are zero:

$$u_{m,-1} = u_{m,1} \quad (m = 0, ..., \infty). \tag{9}$$

The system of Eqs. (6) with the initial and boundary conditions (7)–(9) was solved by the finite difference method. Condition of stability of the finite difference equations is: $\tau \le \min(\sqrt{M/2k_1}, \sqrt{M/2k_2})$.

The calculations of the displacement velocity on the free surface of a block rock mass (n = 0, m = 10, 30) and their spectral densities are shown in Figs. 6 and 7. The load application is at point (0, 0). The other problem parameters: M = 1, $n_1 = -5$, $n_2 = -80$, $L = 1$, $\tau = 0.07$, $\omega_* = 0.9$. Figure 6 illustrates calculations for the uniform half-space ($k_1 = k_2 = 1$), while Fig. 7 demonstrates calculation results for layers of different stiffness: $k_1 = 1$, $k_2 = 9$.

The vertical dashed lines in Figs. 6*a*, *b* and 7*a*–*c* correspond to the wave arrival from the excitation source to points (m, 0) along path 1 as in Fig. 5: $t_1 = m/c_1$. The vertical dash-and-dot line in Fig. 7*a* shows the wave arrival reflected from the boundary $n = n_2$, along path 2: $t_2 \approx \sqrt{m^2/4 + n_2^2}/c_1$. Here, $c_i = L\sqrt{k_i/M}$ (i = 1, 2) are the low-frequency wave velocities in the upper and lower layers. The calculations neglected the wave refraction at the interface of the layers. The double dash-dotted vertical line in Fig. 7*a*–*c* shows the wave arrival time reflected from the boundary $n = n_1$ along path 3: $t_3 = m/c_2 - 2n_1\sqrt{c_2^2 - c_1^2}/(c_1 c_2)$, ($c_2 > c_1$).

It is seen that when $c_2 < c_1$, then, depending on an observer's location, the first comer may be the wave reflected from the two media interface rather than the wave traveling along the shortest path 1. In this case, the velocity amplitude grows by a factor of 2–6 as against the cases $k_1 = k_2 = 1$ and $k_1 = k_2 = 9$. Figure 7*a*–*c* exhibits the propagation of the pendulum wave in the upper layer (dash line) and in the lower layer (double dash-dotted line). The lower, stiffer layer wave overruns the upper layer wave; still, the oscillations are maximal after the arrival of the slower wave of the upper layer. The open mining blasting seismograms are of the same character. The quicker low-amplitude wave comes first, then the slower, small-amplitude wave packet arrives.

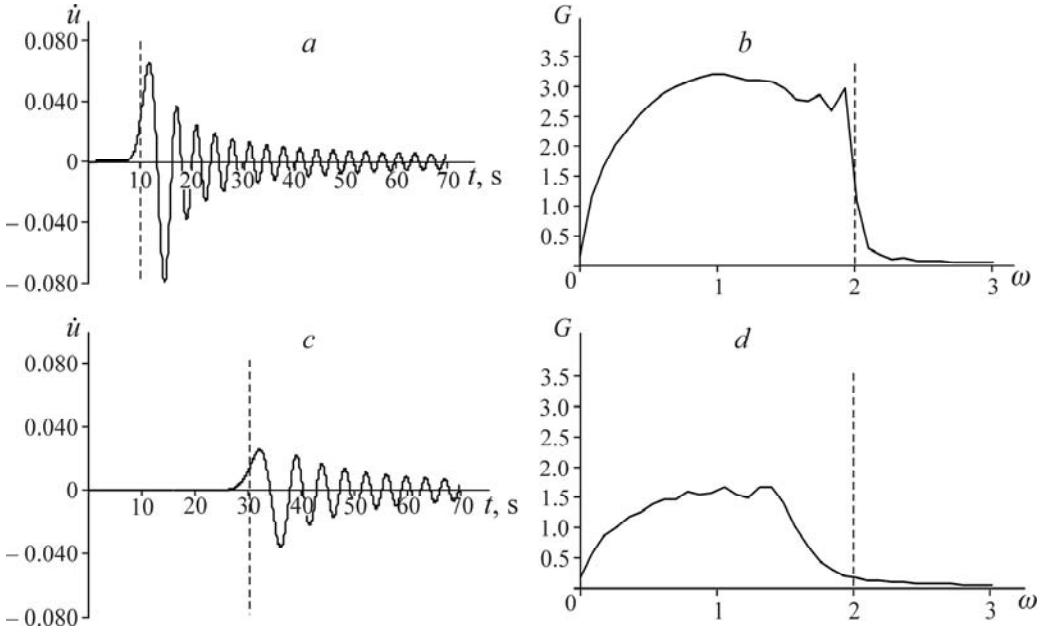

Fig. 6. (*a*, *c*) Velocities of point masses (10, 0) and (30, 0) versus time and (*b*, *d*) their spectral densities G versus frequency under impact loading applied to point mass (0, 0) in the uniform half-space

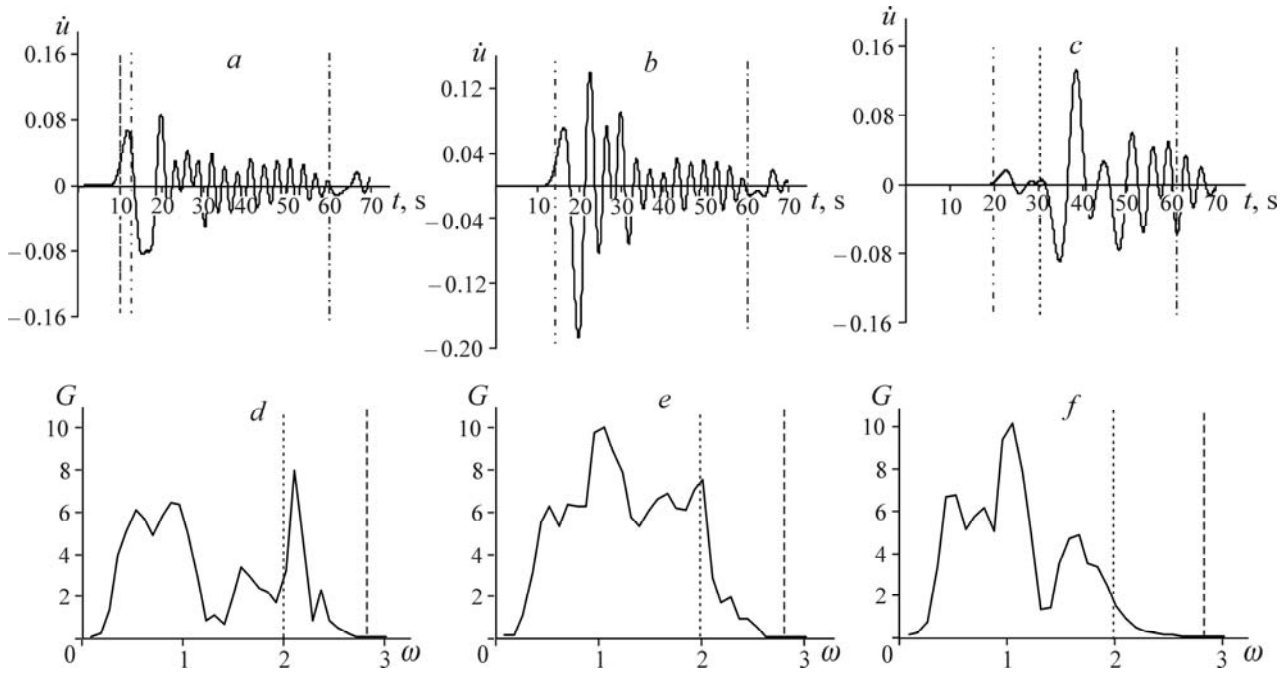

Fig. 7. (*a*, *b*, *c*) Velocities of point masses (10, 0), (14, 0) and (30, 0) versus time and (*d*, *e*, *f*) their spectral densities versus frequency under impact loading applied to point (0, 0) in the layered half-space

Based on the condition $t_1 = t_3$, determine coordinates of the point (m, 0) where 1 and 3 path waves arrive simultaneously:

$$m = -2n_1\sqrt{\frac{c_2 + c_1}{c_2 - c_1}} \ .$$

For the parameters used in the calculations in Fig. 7: $m = 10\sqrt{2}$. The numerical calculations of the velocities at points m = 13, 14, 15, 16 show that the maximum is actually reached at points m = 14, 15 of the concurrent arrival of the upper and lower layer waves. In the other places the waves partially cancel each other. By the calculations, when $c_1 > c_2$, the principal share in the excitation amplitude belongs to the upper layer wave, while the lower layer wave generates the high-frequency oscillations.

Qualitatively, the pattern of wave propagation and spectra in the half-bounded lattice when the load is applied to the free surface of the medium (refer to Fig. 6) fits the behavior of the waves and spectra in a chain of masses [3]: the Airy function describes the mass velocities, the band pass is the same, $0 \le \omega \le 2$.

The comparison of Figs. 6 and 3 shows sufficient differences in the wave propagation in the infinite and half-bounded lattices. There are two resonant frequencies $\omega = 2$ and $\omega = 2\sqrt{2}$ in the infinite lattice and, accordingly, two wave groups run; whereas a single resonant frequency $\omega = 2$ is in the half-bounded lattice with the load application to the free surface and a single wave group with the velocity $c = 1$. Based on the analysis of Fig. 7*d*–*f*, the general share in the spectrum as the wave is propagating is due to the waves travelling in the softer upper layer with the velocity $c = 1$ and frequency $\omega \le 2$.

Figures 8 and 9 present the relationships of the mass velocities, spectral densities and time at the free surface points of the two-layer block medium, the layers having stiffness $k_1 = 1$, $k_2 = 9$. The load application point is $(0,\ n_1)$: $n_1 = -5$, which corresponds to a deep-located excitation source.

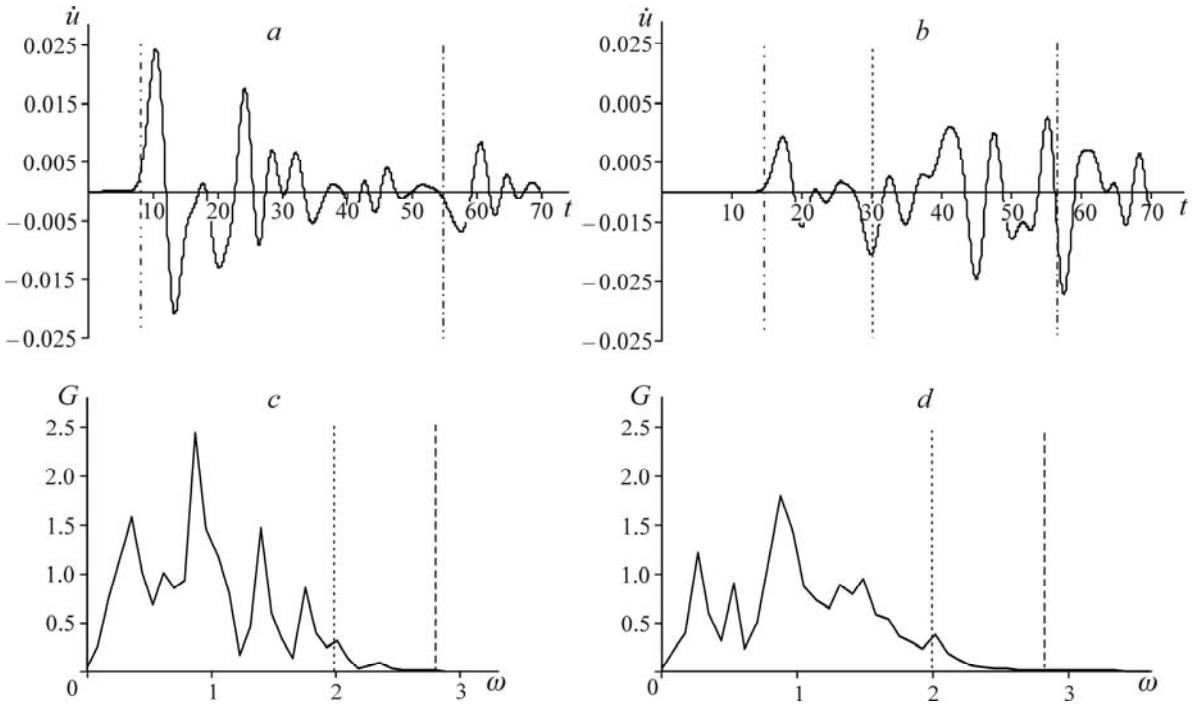

Fig. 8. (*a*, *b*) Velocities of point masses (10, 0) and (30, 0) versus time and (*b*, *c*) spectral densities of these points versus frequency under impact loading application at point mass (0, −5) for the case of $k_1 = 1$, $k_2 = 9$ and $\omega_* = 0.9$

The other parameters are the same as in Fig. 6; the frequencies are $\omega_* = 0.9$, 4.5. The vertical dashed lines in Figs. 8 and 9 show the times of arrival for waves along the paths indicated in Fig. 10.

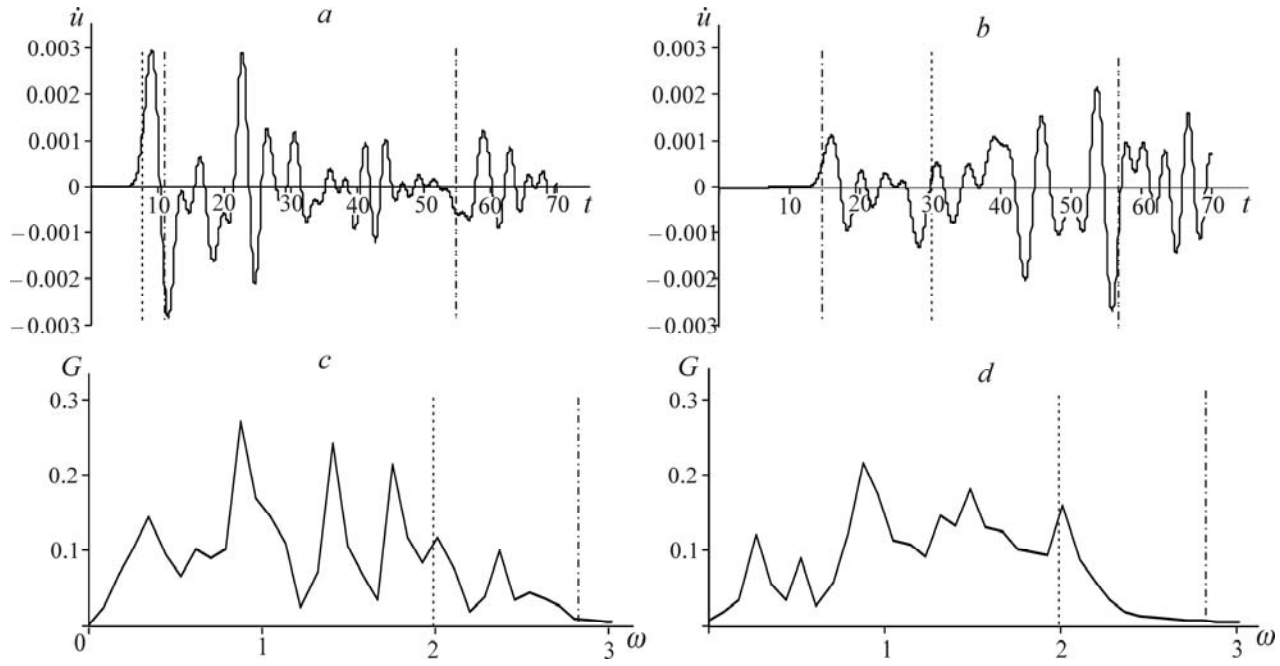

Fig. 9. (*a*, *b*) Velocities of point masses (10, 0) and (30, 0) versus time and (*b*, *c*) spectral densities of these point masses versus frequency under impact loading application at point (0, −5) for the case of $k_1 = 1$, $k_2 = 9$ and $\omega_* = 4.5$

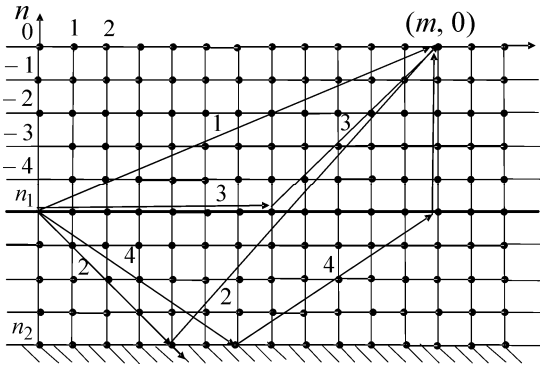

Fig. 10. Layered block medium lattice and passages of seismic wave fronts. Load application point mass is $(0, n_1)$ and observation point mass is $(m, 0)$

The arrival times for the waves propagating along different paths as in Fig. 10 from the excitation source to the observation point are calculated by the formulas of the geometric seismology:

$$t_1 = \sqrt{n_1^2 + m^2}\,/c_1, \tag{10}$$

$$t_2 \approx \left(\frac{2(n_2 - n_1)}{c_2} + \frac{n_1}{c_1}\right)\frac{\sqrt{(2n_2 - n_1)^2 + m^2}}{2n_2 - n_1}, \tag{11}$$

$$t_4 = \frac{2}{c_2}\sqrt{\frac{m^2}{4} + (n_2 - n_1)^2} - \frac{n_1}{c_1}, \quad (c_2 > c_1,\ |n_2| >> m), \tag{12}$$

$$t_3 = \frac{m}{c_2} - \frac{n_1\sqrt{c_2^2 - c_1^2}}{c_1 c_2}, \quad (c_2 > c_1). \tag{13}$$

As follows from the formulas (10)–(13) and Figs. 8, 9, 10, given $c_2 > c_1$, the first comer to the point $(m, 0)$ is the wave running at the interface of the two media (path 3); when $c_2 \le c_1$, the path 1 wave arrives first to the said point. The wave reflected from the lower boundary travels along path 2. With the velocity $c_2 \approx c_1$, the wave path 2 approaches a straight line and the wave travel time is calculated from the formula (11). When $c_2 >> c_1$, path 2 is no more a straight line due to the wave refraction at the interface, and it is possible to replace it by path 4 with calculating the arrival time of the wave reflected from the lower boundary by the formula (13).

The frequency band pass narrows due to the effect of the softer upper layer and is assigned as $0 \le \omega \le 2\sqrt{2k_1/M} = 2.82$, which is supported by the spectral density graphs in Figs. 8 and 9*c*, *d*.

By analyzing the velocity amplitudes in the medium composed of two layers with different stiffnesses, it is obtained that the amplitudes on the free surface are maximal when the lower layer is stiffer than the upper layer.

CONCLUSIONS

1. It has been revealed that the disturbances generated by a local impulse in a 2D regular block medium have a two-wave structure. As in the one-dimensional case, the low-frequency pendulum wave with a unit velocity (velocity of an infinite-long wave in a discrete medium) arrives first at the observation point and is followed up by the high-frequency wave group with the carrier frequency value being close to the first resonant frequency ω_1. The first wave share is practically independent of the signal propagation direction. The high-frequency oscillations are maximal in the diagonal directions.

2. Based on the modeling the blast-induced seismic wave propagation in the two-layer block rock mass, it has been established that the seismic signal shape far away from the excitation source depends on the velocity ratio of the pendulum waves in the layers. If the upper layer velocity is lower, then the small amplitude, stiffer lower layer waves arrives first at the observation point, then comes the maximal amplitude, upper layer, slower wave. The resultant pattern qualitatively agrees with the actual scenarios of blasting at open pits. The arrivals times of the waves are sufficiently accurate calculated within the frames of the geometrical seismology.

The study was conducted with financial support from the Russian Foundation for Basic Research, Project No. 08-05-00509, from the Siberian Branch, Russian Academy of Sciences, Interdisciplinary Integration Project No. 74, and from the Israel Science Foundation, Grant 504/8.

REFERENCES

1. M. A. Sadovsky, "Natural lumpiness of rocks," *Dokl. AN SSSR*, **247**, No. 4 (1979).
2. M. V. Kurlenya, V. N. Oparin, and V. I. Vostrikov, "Formation of elastic wave packets in block medium under impact excitation. Pendulum-type waves V_μ," *Dokl. AN SSSR*, **333**, No. 4 (1993).
3. N. I. Aleksandrova, "Elastic wave propagation in block medium under impulse loading," *Journal of Mining Science*, No. 6 (2003).
4. N. I. Aleksandrova and E. N. Sher, "Modeling of wave propagation in block media," *Journal of Mining Science*, No. 6 (2004).
5. N. I. Aleksandrova, A. G. Chernikov, and E. N. Sher, "Experimental investigation in the one-dimensional calculated model of wave propagation in block medium," *Journal of Mining Science*, No. 3 (2005).
6. N. I. Aleksandrova, A. G. Chernikov, and E. N. Sher, "On attenuation of pendulum-type waves in a block rock mass," *Journal of Mining Science*, No. 5 (2006).
7. M. V. Ayzenberg-Stepanenko and E. N. Sher, "Modeling wave phenomena in media with periodic structures," *Fiz. Mezomekh.*, **10**, No. 1 (2007).
8. E. N. Sher, N. I. Aleksandrova, M. V. Ayzenberg-Stepanenko, and A. G. Chernikov, "Influence of the block-hierarchical structure of rocks on the peculiarities of seismic wave propagation," *Journal of Mining Science*, No. 6 (2007).
9. N. I. Aleksandrova, E. N. Sher, and A. G. Chernikov, "Effect of viscosity of partings in block-hierarchical media on propagation of low-frequency pendulum waves," *Journal of Mining Science*, No. 3 (2008).
10. V. A. Saraikin, M. V. Stepanenko, and O. V. Tsareva, "Elastic waves in block structures," *Journal of Mining Science*, No. 1 (1988).
11. V. A. Saraikin, "Calculation of wave propagation in the two-dimensional assembly of rectangular blocks," *Journal of Mining Science*, No. 4 (2008).
12. Lord Rayleigh, "On the maintenance of vibrations by forces of double frequency, and the propagation of waves through a medium endowed with periodic structure," *Phil. Mag*., **24**, No. 147 (1887).
13. L. Brillouin, *Wave Propagation in Periodic Structures*, NY, Dover Publication (1953).
14. A. A. Maradudin, E. W. Montroll, and G. H. Weiss, *Theory of Lattice Dynamics in the Harmonic Approximation*, NY, Academic Press (1963).
15. D. J. Mead, "Vibration response and wave propagation in periodic structures," *J. Eng. in Industry*, **21**, pp. 783–792 (1971).
16. L. I. Slepyan, *Nonstationary Elastic Waves* [in Russian], Sudostroenie, Leningrad (1972).
17. M. V. Stepanenko and O. V. Tsareva, "Evolution of a shock pulse during its propagation over composite elastic systems," *Journal of Mining Science*, No. 3 (1987).
18. O. A. Luk'yashko and V. A. Saraikin, "Transient one-dimensional wave processes in a layered medium," *Journal of Mining Science*, No. 2 (2007).

19. E. H. Lee and W. H. Yang, “On waves in composite materials with periodic structure, SIAM,” *J. Appl. Math*. (1973).
20. J. Achenbach, “Vibrations and waves in directional composites,” in: *Mechanics of Composite Materials-2*, NY, Academic Press (1975).
21. E. Yablonovitch, “Photonic band-gap crystals,” *J. Phys., Condens. Matter*. (1993).
22. M. Ayzenberg-Stepanenko and L. Slepyan, “Resonant-frequency primitive waveforms and star waves in lattices,” *Journal of Sound and Vibration*, **313**, pp. 812-21 (2008).
23. G. Osharovich, M. Ayzenberg-Stepanenko, and E. Sher, “Unexpected wave-oscillation effects in lattices of regular structure,” in: *The 8th Israeli-Russian Bi-National Workshop 2009 “The Optimization of Composition, Structure and Properties of Metals, Oxides, Composites, Nano and Amorphous Materials”*, **1**, Israeli Academy of Science and Humanities, Jerusalem (2009).